

Micro Structural Investigation On Friction Stir Welded Al–4.5Cu–5TiB₂ Composite

Sreehari Peddavarapu¹ · S. Raghuraman¹ · R. Jayendra Bharathi¹ ·
Gujjalapudi Venkata Sai Sunil¹ · D. B. N. S. Manikanta¹

Received: 14 December 2016 / Accepted: 6 February 2017 / Published online: 22 February 2017
© The Indian Institute of Metals - IIM 2017

Abstract Aluminium matrix composites are widely used in defence and aerospace applications. Welding them is very difficult and is an outstanding issue in a cost effective way. Friction stir welding is a solid state welding technique which is circumventing those barriers and is applied successfully to many such materials recently. In the present work, Al–4.5Cu alloy with TiB₂ reinforcement as in situ which was synthesized by stir casting method was welded by friction stir welding. Threaded pin was used as the friction stir tool profile. One of the joints was found to have tunnel defect in the stir zone due to improper material flow. The microstructural investigation through XRD and SEM revealed that the nugget zone had numerous small particles and refined fine grains which were distributed uniformly and hardness at the welded zone was found to be higher than that of the base material.

Keywords Aluminium matrix composites · Friction stir welding · Threaded pin tool · Nugget zone · XRD · SEM

1 Introduction

Aluminum matrix composites (AMCs) are advanced materials which are used in defense and aero space applications due to their appealing mechanical properties such as stiffness, strength to weight ratio and wear resistance [1–4]. However, the applications of these are limited due to

high production cost and difficulty in fusion welding. Modern advancements in the production of metal matrix composites and novel welding techniques lead to many aerospace applications [2]. Fusion welding of these composites face several problems like solidification shrinkage, less penetration depth, cracks, porosity and work hardening effect producing inefficient joints in terms of strength due to the reaction between reinforcements and matrices leading to the formation of brittle secondary phases in the weld pool or decomposition of reinforcements in molten metal [3–7]. Friction stir welding (FSW) is a solid state welding technique which circumvents these problems. It was invented by ‘The Welding Institute’ at UK in 1991 [4].

The FSW starts with plunging the non-consumable stirring tool into the faying surface of the plates, until the shoulder touches the joint surface and feed is given to the tool along the direction of the joining line. The stirring action of the tool generates enough heat due to frictional action and softens the surrounding material by severe plastic deformation [4]. Further, the material sweeps along with tool surface from advancing side to retreating side as the tool moves further and is deposited at the back of the tool wake in order to form a solid state joint. Feed direction and the rotation of tool (clockwise or anti-clockwise) define the advancing side and retreating side. Plate is in advancing side if the tool feed is in the same direction of the tool rotation, whilst it is in retreating side if they are in the opposite directions. FSW takes place below the melting point of the materials and the maximum temperature attained is 80% of the melting temperature of the work pieces [8]. This welding technique is green and environmentally friendly due to the merits of FSW viz. no gas emission, low energy consumption and no shielding gases which are normally present in fusion welding processes [9]. The strength of the joint is based on the process

✉ Sreehari Peddavarapu
sreehari@mech.sastra.edu

¹ School of Mechanical Engineering, SASTRA University,
Thanjavur 613401, India

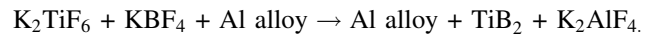
parameters. The process parameters that influence the quality of the welding are rpm of the tool, welding feed, thrust force, tool profile and features, tool material, hardness of the tool etc. [3, 4, 10, 11]. The shape of the tool profile determines the material flow [12, 13]. Swept volume to static volume ratio of the threaded pin profile is equal to 1.01, which assists in superior mixing [14]. Further, the threaded profile pin (TPP) assists for the movement of a severely plastically deformed work piece material around the pin from top to bottom of the joint and vice versa [3]. In the present study, TPP is used to perform the FSW of Al–4.5Cu–5TiB₂ composite which is processed through stir casting method. Microstructural analysis is carried out for both as cast composite and friction stir welded composite with XRD, SEM and EDX maps to analyze the transition across the welded zone. Hardness distribution across the welding section has been studied by Vickers hardness test.

2 Experimental Work

2.1 Preparation of Aluminum Composite

Al–4.5%Cu–5%TiB₂- composite was prepared by stir casting route. It was obtained by an exothermic, in situ, reaction of K₂TiF₆ (109 gm) and KBF₄ (114 gm) salts with molten Aluminum to yield titanium diboride (TiB₂) dispersoids. The pure Aluminum (commercial) ingots were cut to suitable size, using power saw so as to accommodate in graphite crucible, and dilute HCl was used for pickling the small pieces of Aluminum followed by thorough cleaning with acetone to remove any grease or any other oily contaminants. The requisite amount of K₂TiF₆ and KBF₄ salts, to yield the required wt% of TiB₂ was weighed and subsequently dried separately in an oven at 150 °C for one hour in order to drive out any physisorbed moisture present. Once the drying was completed, the salts were mixed thoroughly in order to get homogeneous mixture, and the powder mixture was wrapped in Aluminum foil into number of small batches to form packets of convenient size and kept ready to be added to liquid alloy. The master alloy was remelted with suitable amount of Aluminum in a pit type resistance furnace using a graphite crucible, coated with zirconia paste and dried well to prevent the contamination of melt with carbon from the crucible during melting, so that an alloy with the desired composition could be obtained. The temperature of the melt was raised to the predetermined reaction temperature of 800 °C, and degassing of the melt was carried out by adding the hexachloroethane (C₂Cl₆) tablets. The degassing was accompanied by a slight drop in temperature. Once the melt attained the set temperature again, the salt mixture was then added in batches and the melt was stirred with a zirconia coated

graphite rod for uniform mixing. The entire mixture was held at the reaction temperature for one hour from the time of addition of salts in order to ensure complete reaction. Intermittent stirring of the melt was carried out for every 10 min in order to ensure good distribution of the salt in the molten Aluminum to ensure uniform reaction throughout the melt. TiB₂ particles were formed in situ inside the molten Aluminum through the reaction of K₂TiF₆ and KBF₄ salts following the equation.



The K₂AlF₄ floats up as dross and was subsequently removed. The melt was subsequently stir-casted by top pouring into plate-shaped cast iron mould which was preheated to about 200 °C.

2.2 Friction Stir Welding of Composites

The cast composites were machined to the size of 70 × 35 × 6 mm and friction stir welding was carried out on the converted vertical milling machine and the set up is shown in Fig. 1. Work pieces were cleaned through acetone and clamped on the fixture to fit the plates together to carry out FSW. The welding tool material was selected as M2 steel which was hardened to 62HRC. The tool consisted of threaded (M6x1p) pin profile with the required dimensions to fit on to the machine spindle as shown in Fig. 1.

The FSW process was initiated by plunging the tool into the faying faces of the work piece followed by Stirring action which plastically deformed the material and sweeps along with tool surface from advancing side to retreating side and deposited at the back of the trailing edge to form a solid state joint through extrusion and forging. The tool was removed from welded composite before the tool reached the leading edge on the joint which left the hole on the work piece [4]. FSW was carried out at tool rotation speed of 710, 1000 and 1400 rpm at a constant feed rate (welding speed) of 63 mm/min.

3 Results and Discussion

3.1 As-Cast Composite

3.1.1 XRD Analysis

Al–4.5%Cu–5%TiB₂ composite was synthesized by stir casting process successfully. Fig. 2a, presents the XRD pattern from the as-cast Al–4.5Cu–5TiB₂ composite, showing the peaks of Al, CuAl₂, and TiB₂ and absence of the precursor salts conform the completion of reaction [15] leading to the formation of TiB₂ particles during in situ

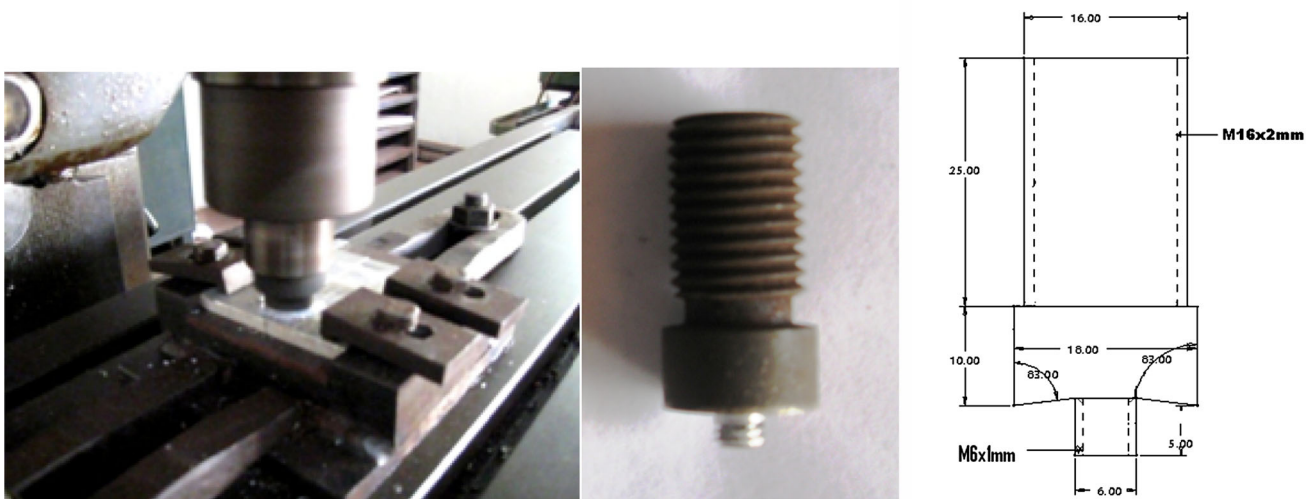


Fig. 1 Friction stir welding setup showing threaded profile tool with dimensions

processing. No evidence for formation of the brittle intermetallic phase, Al_3Ti has been observed which suggests that possibly Al_3Ti is not there.

3.1.2 SEM Analysis

Microstructural characterization of the composite has been carried out with SEM and EDX maps. Figure 2b–f shows the SEM BSE image of the composite and EDX maps of Al, Ti, and Cu, respectively. The EDX map of Ti in Fig. 2e and the absence of peaks belonging to Ti-containing phases other than TiB_2 in the XRD pattern (Fig. 2a), conform that the particles appearing bright are TiB_2 only [15]. Both the SEM image (Fig. 2b) and X-ray map of Ti in Fig. 2e reveal that the TiB_2 particles are located primarily at grain boundaries in the as-cast structure. In another investigation on as-cast in situ Al– TiB_2 composites processed through mixed salt route [16], have also reported about the location of particles at grain boundaries. Observation reveals that TiB_2 particles are reasonably well dispersed in the matrix. Agglomeration of hard particles which leads to reduction in toughness of the composite is a common defect that has been observed in [3, 17], But it is not observed in the cast composite.

3.2 Friction Stir Welded Composite

3.2.1 XRD Analysis

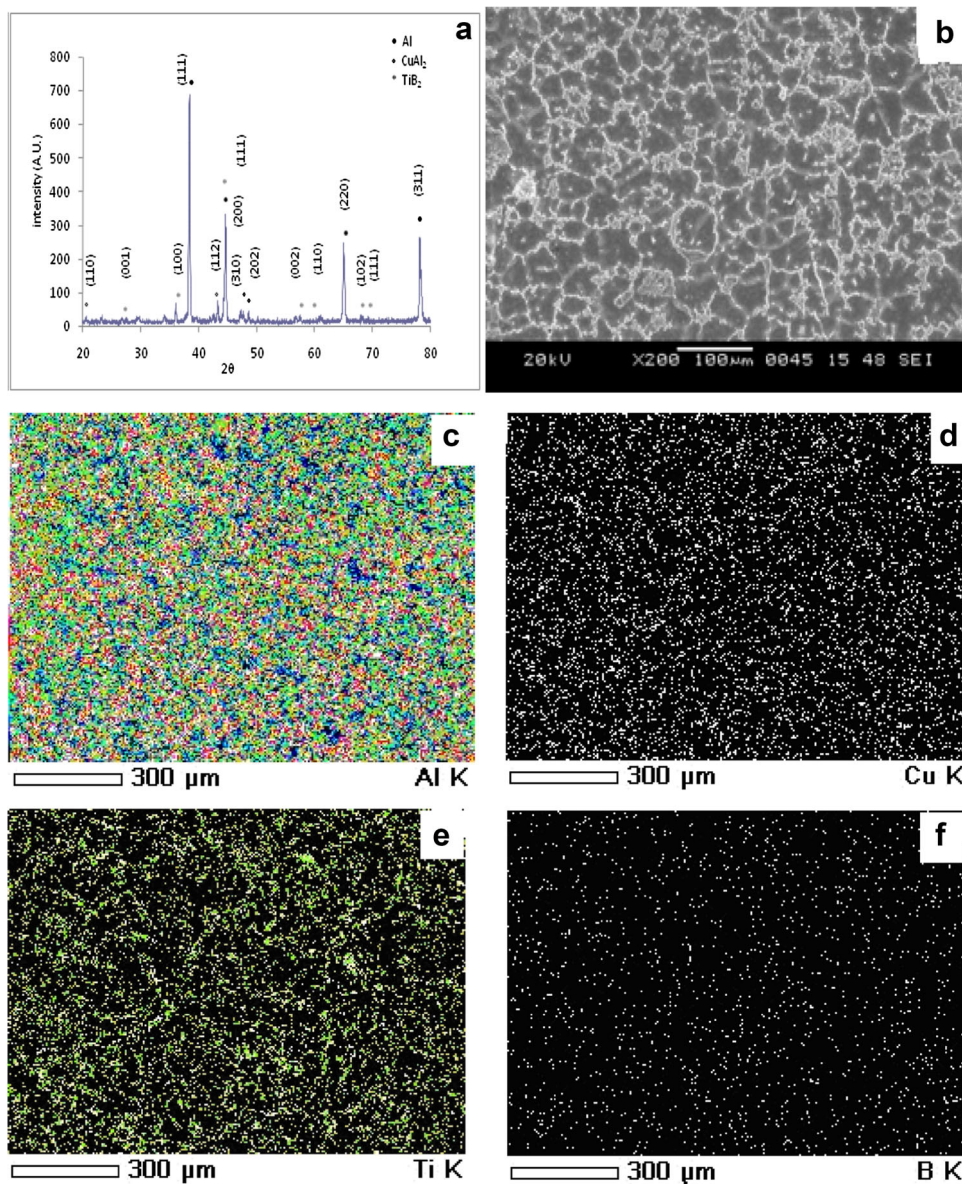
Figure 3a, presents the XRD pattern from the friction stir welded Al–4.5Cu–5 TiB_2 composite, showing the peaks of Al, $CuAl_2$, and TiB_2 . As is in as cast composite, no evidence of formation of the brittle intermetallic phase, Al_3Ti is observed which suggests that possibly Al_3Ti is not there.

3.2.2 SEM Analysis

Al–4.5%Cu–5% TiB_2 composite has been joined successfully by friction stir welding with rotational speed of 1400, 1000 and 710 rpm and at a constant feed rate of 63 mm/min, as shown in Fig. 4a–c using TPP tool. The tunnel defect is observed (Fig. 4c) on the work piece welded at 710 rpm. This may be due to improper penetration of the tool to the root or insufficient material movement from tool rotation [4]. Figure 3b–f are the SEM BSE images of the composite and EDX maps of Al, Ti, and Cu, respectively. The EDX map of Ti in Fig. 3e and the absence of peaks belonging to Ti-containing phases other than TiB_2 in the XRD pattern (Fig. 3a), conform that the particles appearing bright are TiB_2 only, as has been the case for as-cast composite.

The stirring action of the tool produces severe plastic deformation at the weld center resulting in equiaxed fine grain structure. The microstructure is altered significantly in the weld center as compared to that of the base material. SEM image presented in Fig. 4d shows the transition from base material to weld center. Based on the micro structure developed at the weld region of the composite, it can be divided into four zones: (a) Base Material (BM), (b) Heat affected zone (HAZ), (c) Thermomechanically affected zone (TMAZ), and (d) Nugget Zone/Stirring zone (NZ) [3, 13]. The change in microstructure mainly depends on severe plastic deformation and frictional heat generated due to stirring action of the tool, generates high strain which lead to rearrangement of TiB_2 particles and precipitates, from agglomerates at the grain boundary in the base material to homogeneous distribution in the NZ of welded specimen [13]. Smaller and equiaxed grains are observed in the NZ (Fig. 3b), resulting from the mechanism of

Fig. 2 **a** XRD pattern showing the peaks of Al, TiB_2 and CuAl_2 in as cast Al–4.5Cu–5 wt% TiB_2 composite. **b** SEM image showing rosette-like dendritic grain structure in as cast Al–4.5Cu–5 wt% TiB_2 composite. **c–f** SEM (BSE) micrograph showing TiB_2 particles at grain boundaries, and EDX maps of: Al, Cu, Ti and B



constant dynamic recrystallization [18, 19]. There is a reduction in size of TiB_2 particles and precipitates due to abrasive action of the tool and collision of hard particles with each other [4, 16]. In the region of TMAZ, highly elongated grains (Fig. 4d) [4, 20] have been observed. This may be due to the combined action of plastic deformation and heat [21] which has resulted in insufficient strain and heat to form recrystallization [22]. In HAZ, there is no influence of plastic deformation and the material experiences only heat. The increase in temperature lead to softening due to grain growth and increase in grain size. In BM, since there is no influence of both plastic deformation and heat, the grain size remains unchanged.

3.2.3 Hardness Distribution at Welded Region

The Vickers hardness distribution of the friction stir welded composite joint obtained across the transverse section at different rotational speed for a constant welding feed is shown in Fig. 5. The hardness is a function of grain size, dislocation density, hard reinforcing particles, and welding process parameters. However, the hardness distribution along the weld zone is W-shaped [23]. All the composite joints show higher hardness value at NZ as compared to base material. The reason behind increase in hardness may be two folds. Finer grain sizes, result in higher hardness according to theory of Hall–Petch [24] and Pinning of several small TiB_2 particles at the grain boundary [25].

Fig. 3 **a** XRD pattern showing the peaks of Al, TiB₂ and CuAl₂ in friction stir welded Al–4.5Cu–5 wt% TiB₂ composite **b** SEM image showing fine grains of NZ. **c–f** EDX maps o: Al, Cu, Ti and B

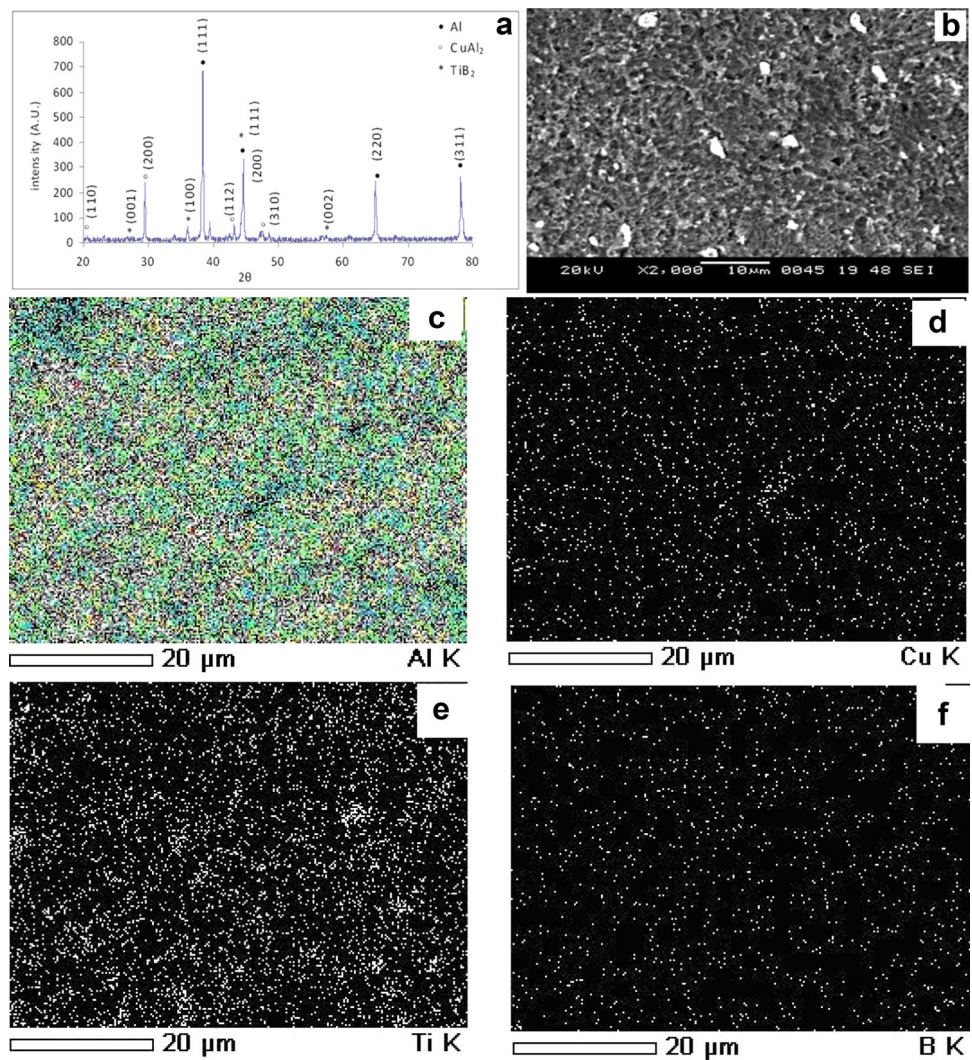
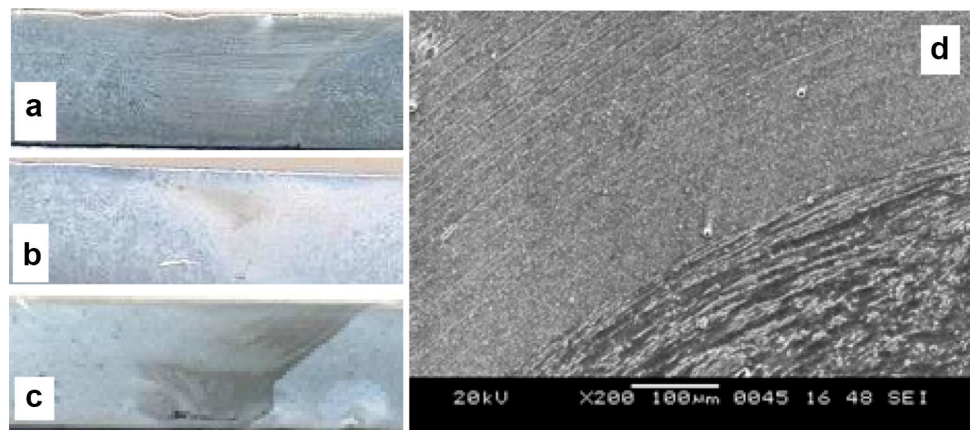


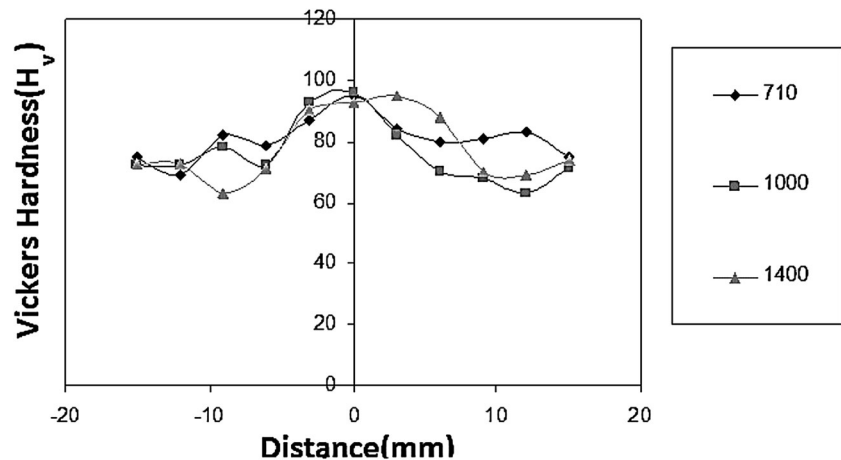
Fig. 4 **a–c** Friction stir welded work pieces; **d** Transition zone



Numerous small TiB₂ particles are produced by abrasive action of the tool and striking of hard particles to each other. They are distributed homogeneously in NZ, and they contribute to increased hardness [3]. Lower hardness value is observed in the Heat affected Zone (HAZ). This is

mainly due to grain softening induced by the thermal effect during stirring of the material by the tool. From Fig. 5, it is observed that as the welding speed increases, the hardness is increased. The welding speed decided the time of exposure of frictional heat between the tool and the base

Fig. 5 Hardness distribution across the weld



material interface per unit length. The more the time of frictional heat exposure, the more is the heat supplied which eventually affect the grain growth [26]. The small increase in the hardness is due to decrease in the quantity of heat supplied which lead to the formation of fine grains. The highest hardness is obtained for rotational speed of 1000 rpm, which is higher than the hardness obtained for rotational speed of 710 rpm. Increase in the tool rotational speed leads to increase in heat generation and also proper stirring of the materials at NZ. Heat gain at rotational speed of 1400 rpm causes the grain refinement, leading to decrease in hardness [26]. Lower rotational speed results in lower heat condition and lower stirring effect which leads to improper consolidation of material at weld zone [3].

4 Conclusions

The Al–4.5%Cu–5%TiB₂ composite were successfully synthesized by stir casting process. The influence of tool rotational speed on microstructure and hardness of Friction Stir Welded composite was investigated. Tunnel defect was observed at the root of the NZ for the lower rpm of the TPP tool. The microstructural behavior of the weld zone exhibited homogeneous distribution of fine recrystallized grains with numerous small TiB₂ particles and precipitates being found at the NZ due to stirring action of the tool and collision of hard particles to each other. Elongated grains were observed at TMAZ. The NZ hardness was higher than that of base material due to grain refinement and small hard particles.

References

1. K Suryanarayanan, R Praveen, and S Raghuraman, *Int J Innov Res Sci Eng Technol* **2** (2013) 11.
2. A Kumar, C Veeresh Nayak, M A Herbert, and S S Rao, *Mater Res Innov* **14** (2014) 84.
3. M A Herbert, A K Shettigar, A V Nigalye, and S S Rao, *Mater Sci Eng* **114** (2016) 012125.
4. O S Sali, H Ou, W Sun, and D G McCartney, *Mater Des* **86** (2015) 61.
5. A M Hassan, M Almomani, T Qasim, and A Ghaithan, *Mater Manuf Process* **27** (2012) 1419.
6. M B D Ellis, *Int Mater Rev* **41** (1996) 41.
7. R Y Huang, S C Chen, and J C Huang, *Metall Mater Trans A* **32** (2001) 2575.
8. B Ashish, J S Saini, and B Sharma, *Trans Nonferrous Met Soc China* **26** (2016) 2003.
9. E T Akinlabi, and S A Akinlabi, *World Acad Sci Eng Technol* **71** (2012).
10. Nami H, H Adgi, M Sharifitabar, and H Shamabadi, *Mater Des* **32** (2011) 976.
11. K Kalaiselvan, and N Murugan, *Trans Nonferrous Metal Soc China* **23** (2013) 616.
12. B A Kumar, and N Murugan, *Mater Des* **57** (2014) 383.
13. S J Vijay, N Murugan, *Mater Des* **31** (2010) 3585.
14. P Periyasamy, B Mohan, V Balasubramanian, S Rajakumar, S Venugopal, *Trans Nonferrous Metal Soc China* **23** (2013) 942.
15. M A Herbert, R Maiti, R Mitra, and M Chakraborty, *Solid State Phenom* **116** (2006) 217.
16. S Lakshmi, L Lu, M Gupta, *J Mater Proc Tech* **73** (1998) 160.
17. D Storjohann, O M Barabash, S S Babu, S A David, P S Sklad, and E E Bloom, *Metall Mater Trans A* **36** (2005) 3237.
18. AH Feng, B L Xiao, and ZY Ma, *Compos Sci Technol* **68** (2008) 2141.
19. J Q Li, H J Liu, *Mater Des* **45** (2013) 148.
20. H Khodaverdizadeh, A Mahmoudi, A Heidarzadeh, E Nazari, *Mater Des* **35** (2012) 330.
21. W F Xu, J H Liu, D L Chen, G H Luan, and J S Yao, *Mater Sci Eng A* **548** (2012) 89.
22. M S Khorrani, M Kazeminezhad, A H Kokabi, *Mater Des* **40** (2012) 364.
23. A K Shettigar, G Sali, M Herbert, S Rao, *Def Sci J* **63** (2013) 429.
24. M Bahrami, M K B Givi, K Dehghani, and N Parvin, *Mater Des* **53** (2014) 519.
25. A Shamsipur, SF Kashani-Bozorg, A Zarei-Hanzaki, *Surf Coat Technol* **206** (2011) 1372.
26. R Palaanivel, P K Mathews, N Murugan, and I Dinaharan, *Procedia Eng* **38** (2012) 578.